

**APPENDIX 1****GAM Environmental Layer extraction:**

Bathymetry data were downloaded from the British Columbia Marine Conservation Analysis (BCMCA) webpage\*, with a spatial resolution of 100 m. We later derived the slope from the Bathymetry using the *Spatial Analyst Slope* tool in ArcGIS. We also derived Terrain Ruggedness from the bathymetry layer, using the *Benthic Terrain Modeler 3.0* tool (Walbridge et al. 2018). Bathymetry, slope, and ruggedness were all aggregated to the 4 km<sup>2</sup> grid cell and saved as raster GeoTiff files.

We extracted tidal current information from modeled values generated by Foreman et al. (2008), with all data downloaded from the BCMCA website. The tidal speed values used are the average root mean square tidal speeds over many tidal cycles.

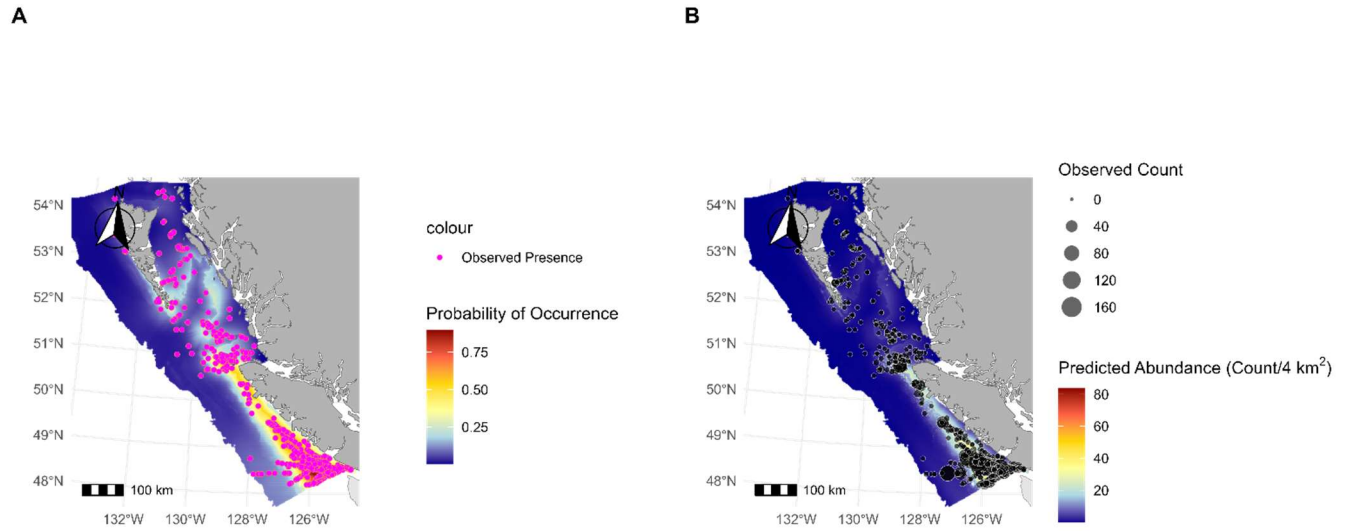
To calculate the distance to the shelfbreak, we used the *Near* tool in ArcGIS pro to calculate a given distance from a grid cell centroid to the 200-m isobath (shelfbreak) and then saved as a raster using the points to raster tool. We used the spatial join tool in ArcGIS to determine if a grid cell was on or off the shelfbreak. With a value of 1 symbolizing a point being on the shelf and 0 equating to being off. These points were converted to a raster layer using the points to raster tool.

We downloaded sea surface temperature (SST, °C) from the National Oceanic and Atmospheric Administration Coral Reef Watch program. We resampled the SST rasters in R to match our grid spatial scale. SST fronts were calculated from the SST rasters using the Marine Geospatial Ecology Tools (MGET) Cayula Cornillon Single Image Edge Detection algorithm (version 0.8a75). Monthly SST raster images were used to calculate the fronts on a monthly basis (May to October) between 1992 and 2019. We applied the MGET Cayula Cornillon Single Image Edge Detection algorithm for each SST raster image, using a histogram window stride of 16 and window size of 32. The resulting raster is of a binary image with 1's representing fronts and 0's representing all other water pixels in the study area. We then used the distance function from the raster package in R to calculate the distance from grid centroid to the grid centroid. The average SST and the average distance to SST fronts was calculated from these monthly layers.

Submarine Canyons were extracted from the inventory shape file created by Harris and Whiteway (2011). The distance of centroid points to the nearest marine canyon was calculated to grid cell centroids and then saved as a raster layer.

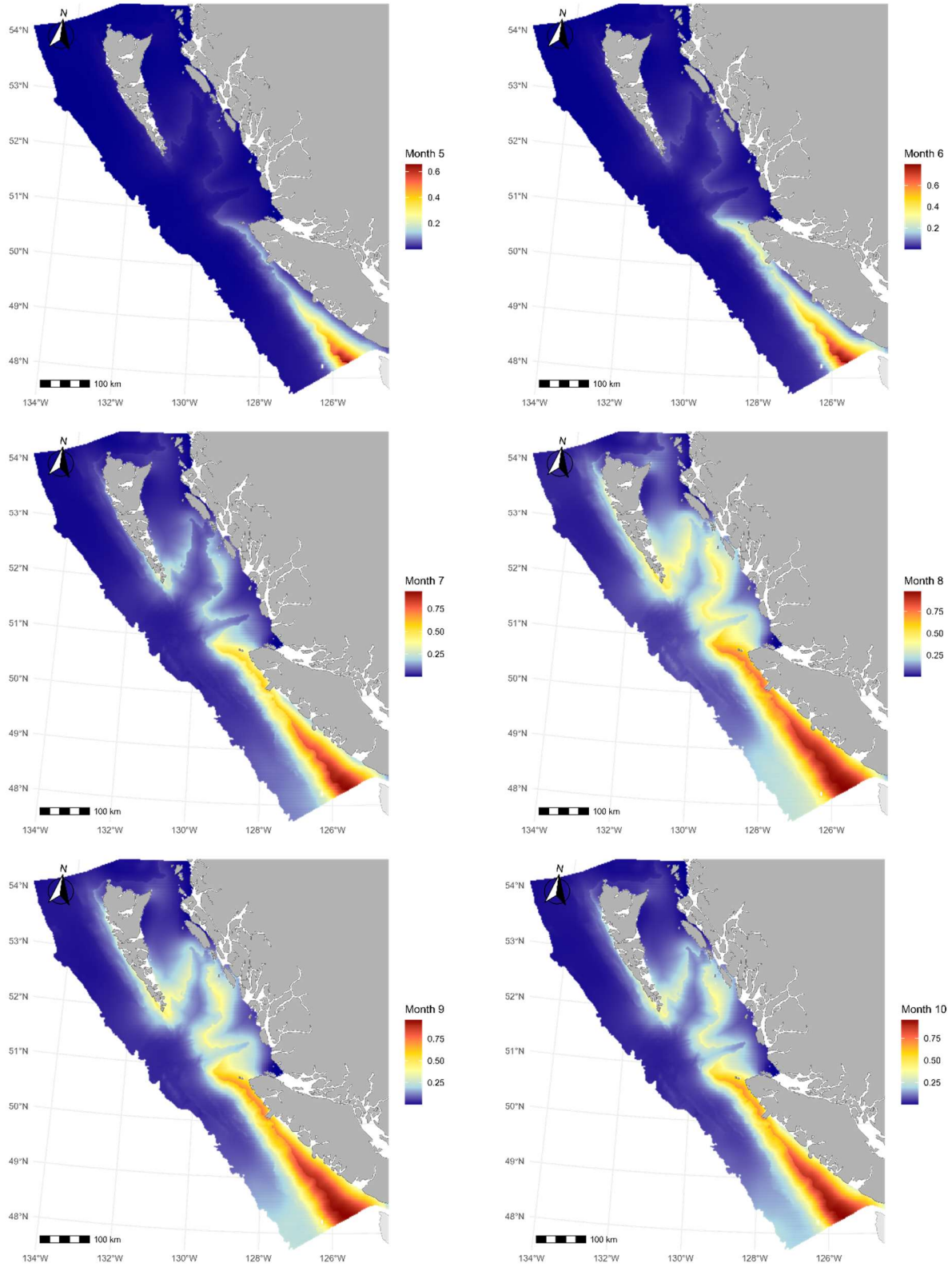
Once all layers were extracted and saved as raster files, we stacked them in R and extracted them to the observation dataset and to the spatiotemporal prediction dataset. The prediction dataset contained coordinates for the centroid 4 km<sup>2</sup> grid cells within our study region. Points were repeated for the months May to October, between 1992 and 2019.

\*[https://bcmca.ca/datafeatures/eco\\_physical\\_hightidalcurrent](https://bcmca.ca/datafeatures/eco_physical_hightidalcurrent)



37

38 **Fig. A1.** Average predicted probability of Pink-footed Shearwater presence, derived from the presence-absence GAM model and  
39 projected onto a 4 km<sup>2</sup> grid, overlaid with Pink-footed Shearwater occurrence points represented from the centroids of transects  
40 birds were seen on. Average predicted relative abundance of Pink-footed Shearwaters, derived from the 2-step GAM model and  
41 projected onto a 4 km<sup>2</sup> grid, overlaid with Pink-footed Shearwater occurrence points represented from the centroids of transects  
42 birds were seen on.



43

44 **Fig. A2.** Average predicted probability of Pink-footed Shearwater presence, by month, derived from the presence-absence GAM  
45 model and projected onto a 4 km<sup>2</sup> grid.

- 46 Foreman, M. G. G., Crawford, W. R., Cherniawsky, J. Y., Henry, R. F., & Tarbotton, M. R.  
47 (2000). A high-resolution assimilating tidal model for the northeast Pacific Ocean. *Journal of*  
48 *Geophysical Research: Oceans*, 105, 28629–28651.
- 49 Harris, P. T., & Whiteway, T. (2011). Global distribution of large submarine canyons:  
50 Geomorphic differences between active and passive continental margins. *Marine Geology*,  
51 285(1–4), 69–86.
- 52 Walbridge, S., Slocum, N., Pobuda, M., & Wright, D. J. (2018). Unified geomorphological  
53 analysis workflows with Benthic Terrain Modeler. *Geosciences*, 8(3), 94.
- 54